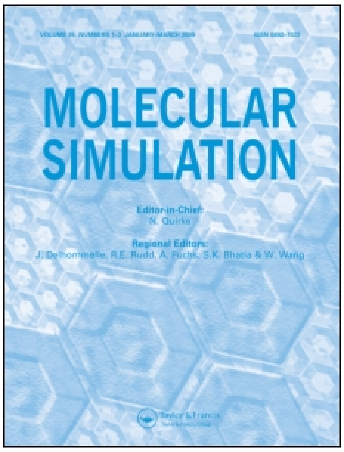

Molecular Simulation
Publication details, including instructions for authors and subscription information:
http://www.informaworld.com/smpp/title~content=t713644482

Modeling the effects of particles, interstitials, vacancies and tip geometry on indentation-induced plasticity

S. Mukherjee[a]; T. Khraishi[a]; Y. -L. Shen[a]
[a] Department of Mechanical Engineering, University of New Mexico, Albuquerque, NM, USA

To cite this Article Mukherjee, S. , Khraishi, T. and Shen, Y. -L.(2006) 'Modeling the effects of particles, interstitials, vacancies and tip geometry on indentation-induced plasticity', Molecular Simulation, 32: 8, 651 — 656
To link to this Article: DOI: 10.1080/08927020600891437
URL: http://dx.doi.org/10.1080/08927020600891437

Molecular Simulation, Vol. 32, No. 8, 15 July 2006, 651–656

Modeling the effects of particles, interstitials, vacancies and tip geometry on indentation-induced plasticity

S. MUKHERJEE, T. KHRAISHI* and Y.-L. SHEN

Department of Mechanical Engineering, University of New Mexico, Albuquerque, NM 87131, USA

(Received April 2006; in final form May 2006)

In this work, which is a follow-up of an earlier work by the authors in this journal, we discuss the effects of particles, interstitials, vacancies and indenter-tip geometry on indentation-induced plasticity. A nano-indentation model based on a close-packed array of straws was used. Upon indentation with a cylindrical indenter, the results observed *in situ*, match qualitatively computer atomistic and finite-element simulation models. This model helps explain the phenomenon and physical reasons for annihilation of vacancies. It also shows the strong effect of interstitials on the inception of plasticity at their sites. It shows that a rigid particle acts as a stress concentrator even away from the indenter. On indentation with a flat indenter, curling of atoms at the indenter edges was observed, along with slip lines reported in the literature.

Keywords: Vacancies; Interstitials; Particles; Nanoindentation; Plastic deformation

1. Introduction

In an earlier work by our group [1], a straw model was presented as an alternative to the Bragg–Nye bubble raft model [2]. It is comprised of an array of close-packed straws coated with glycerin and housed in a Plexiglas box. A cylindrical indenter was used to indent the assemblage from its top free surface at a chosen rate of $0.1''$ per minute till plasticity was induced.

As indentation progressed in the defect-free structure, it was initially observed that the top layers of atoms were compressed beneath the indenter and the array of straws deformed elastically up to a certain limit. Upon further indentation, significant movement of atoms occurred as dislocations were created. These dislocations moved initially along "V"-shaped tracks conforming to observations from the Bragg–Nye bubble raft model [2]. The preferred movement of dislocations is along the slip directions with the expected highest resolved shear stress [3–6]. It was observed that the preferred slip directions were along 60° and 120° inclinations and the two dislocation slip paths have a 60° angle between them as observed in the earlier models [2,4]. On further indenting the array, it was observed that the dislocations impinge on the free surface and form either slip-steps [3,5] or pile-ups [7–10].

In this paper, we introduce defect sites, at locations of choice, in the form of vacancies and interstitials. We also introduce rigid particles. Upon indentation with a circular indenter, our observations qualitatively agree with computer simulation results performed previously by our research group [11,12] and here. Also, when indenting with a flat indenter, we observed similar atomic movement to that described by classical continuum plasticity models [13].

Thus our defect simulation model, apart from being experimental, *in situ*, inexpensive and easy to set-up, also allows different sizes of defects or particles to be placed at locations of choice, along with the flexibility of changing the indenter geometry. Furthermore, it can simulate either plane-stress or plane-strain conditions by varying the straw length. The latter, along with the capability of simulating second-phase or reinforcement particles is the main advantage of the straw model over the bubble-raft model. The main advantage of this model over traditional continuum finite-element simulations is the ability to observe nano-scale phenomena associated with plasticity generation (due to the discreteness of the model). Another advantage is the ability to observe the formation of voids and to undergo large deformations. The last two can be attained with computer atomistic simulations, which our model is closest to in capability. The main disadvantages

*Corresponding author. Tel.: + 1-505-277-6803. Email: khraishi@me.unm.edu

Molecular Simulation
ISSN 0892-7022 print/ISSN 1029-0435 online
http://www.tandf.co.uk/journals
DOI: 10.1080/08927020600891437

of computer atomistic simulations are the time and know-how involved in setting up the model and running it. Finally, it is also possible to record a load-displacement curve for the suggested straw model, similar to real nano-indentation experiments. The presented results below do not show such a curve due to the large load-cell attached to our instrumentation. Future plans revolve on obtaining a smaller load-cell capable of accurately recording the small forces involved in indenting the straw model.

2. Method

Drinking straws are cut to an equal size and surface coated with commercially available glycerin. These straws simulate atoms in nano-indentation experiments and glycerin mimics the inter-atomic forces, which helps hold the atoms together. The tension provided by glycerin has been found to hold for many days under typical ambient conditions. These straws are stacked to resemble a (111) FCC close-packed plane. A detail of the model set-up is available in an earlier paper [1]. This plane of atoms can be indented from its top free surface. Atom movement on the sides and bottom of this assembly is confined by Plexiglas walls.

A vacancy site is created in the close-packed plane by withdrawing a straw piece from the original array. Thus, the vacancy size is equal to the diameter of one straw. Care must be taken when withdrawing a straw, as the glycerin coating its surface tends to pull with it its nearest neighbors out. The nearest neighbors would have to be continuously tapped in place. Once a vacancy is created this way, the neighboring atoms would not fill its site due to their close packing and it will stay as is.

An interstitial site was formed by introducing a small-diameter straw into the crevice in between three nearest-neighbor larger straws. Naturally, if the small straw (e.g. impurity atom) is larger than the space provided by the crevice, there will be a local disturbance in the atomic structure around the interstitial. The disturbance extent and magnitude will thus depend on the interstitial size. In this case, we use an interstitial-to-straw ratio equal to 0.417.

Particles were made by filling a number of straws with candle wax. These straws were then glued together on their touching surfaces. In this manner, it is possible to achieve particles of different geometry and size. In the current work, a hexagonal-shaped particle composed of seven wax-filled straws was made. Since wax is much more rigid than air, such particles are considered rigid compared to the rest of the array straws. The rigidity of such particles can be controlled by varying the filler material.

All the above defects can be introduced at the site of choice in the close-packed array. Here, it is worth noting that no observable structural relaxation was seen due to the creation of a vacancy or the insertion of hexagonal-shaped particles. This is mostly because these defects do not represent a misfit in the crystal structure. In the case of the interstitial, however, structural relaxation of the straws can be observed over a period on the order of a second.

A tensile/compression Instron machine then lowers the indenter at a chosen rate of 0.1″ per minute until plasticity ensues in the model. The indenter for the nano-indentation experiment is either a cutout from an 8-inch cylinder or a flat slab, both having a width of approximately 1″ to match the length of the straws and thus model two-dimensional (2D) conditions. The indenter is gripped to the jaw of the Instron machine through a metallic pin. A digital video camera was used to record all the experiments in order to ensure that the results are available for post-experiment analysis and review. The camera view was set-up perpendicular to the plane of the straws.

3. Results and discussion

As indentation progressed, in the defect-free structure, the top layers of atoms were initially compressed beneath the indenter. While the array of straws was deforming elastically, zones of compression and tension were identified (figure 1). The identification occurred via visual inspection by monitoring changes in straw diameter or spacing between straws. These tension and compression zones will be revealed more clearly in subsequent discussions as a result of the performed finite-element simulations.

We introduced defects (vacancies and interstitials) and particles in these areas and recorded their effect on the indentation-driven plasticity, the results of which are presented below.

3.1 Vacancies

With regard to vacancies, we observe squashing of these vacancies in the compression zone during elastic deformation. Rows of atoms are seen moving towards the squashing vacancy (figure 2) and eventually plug the hole. In an earlier computer simulation work [11], it was observed that vacancies get plugged or annihilated by the movement of an atomic row towards them, which is consistent with the current work.

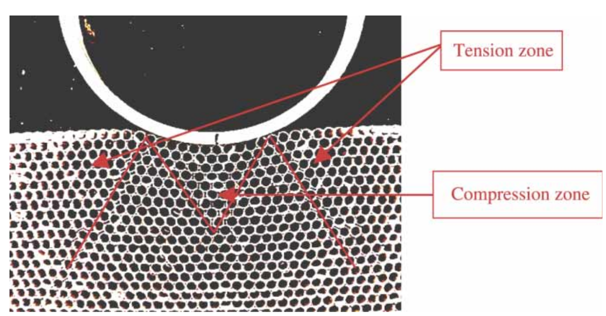

Figure 1. Indentation of a close-packed plane of straws using an 8-inch indenter and showing regions of compression and tension.

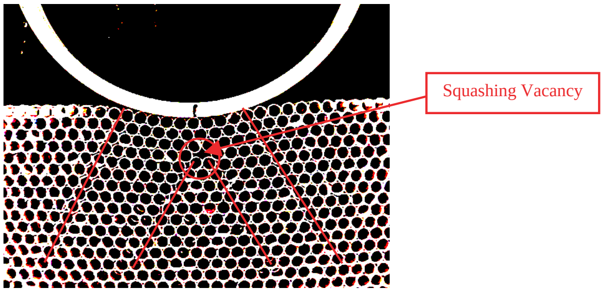

Figure 2. Rows of atoms move towards a vacancy and eventually plug (annihilate) it.

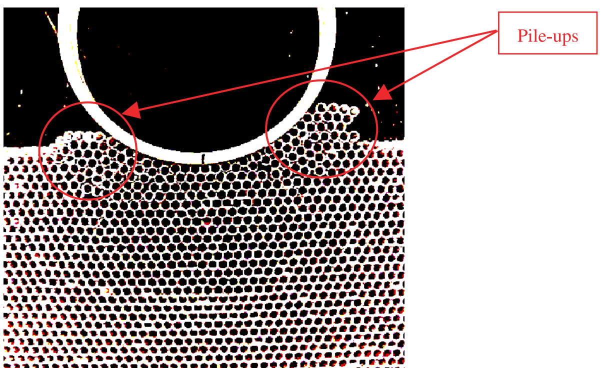

Figure 3. Pile-ups form at the free surface and crystal order restored under the indenter. The vacancy here being totally annihilated in the compression zone.

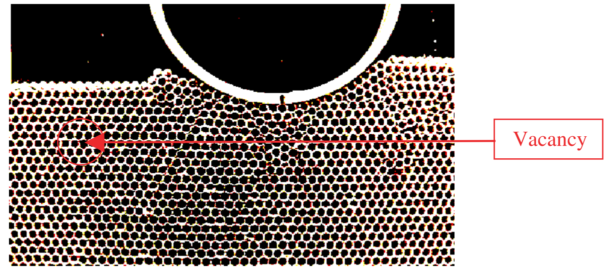

Figure 5. Vacancies located far away from the indenter do not seem to have any effect on plasticity occurring underneath the indenter.

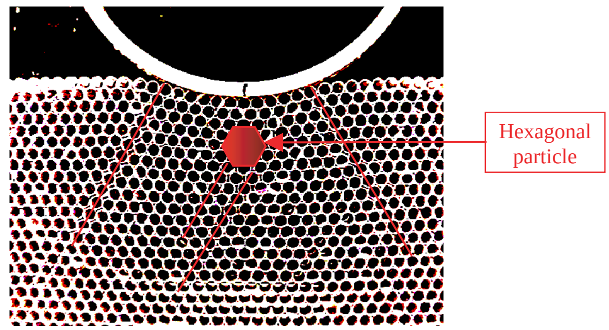

Figure 6. The particle transmits strain beneath it at an angle to the indentation axis.

Vacant sites present in the compression zone, near and directly underneath the indenter axis, get annihilated as plasticity ensues (figure 3). Again, this is similar to what has been reported in [11]. In the tension zones of the crystal, the vacant sites tend to enlarge as opposed to compress (which is what happens in the compression zone, figure 4). Vacancies located far away in the crystal do not seem to have any effect on the plasticity occurring underneath the indenter (figure 5), i.e. the vacancy site experiences no local plasticity or significant atom motion.

3.2 Particles

The particle present in the compression zone, near the indenter, exhibits atom movements (slanted with respect to the indentation axis) below its position (figure 6). Such particle-induced strain was evident, in a similar trajectory, from contour plots using finite-element simulations on particulate composite material [12]. When the particle is placed along the main shear lines indicated in figure 1, the particle inhibits any sliding of atoms crossing its path which results in plastic deformation on the other end of contact away from the particle. This intuitive result was observed repeatedly no matter on which side of the indentation the particle resided (figure 7). Particles placed away from the indenter but close to the main slip regions (noted earlier in figure 1) seem to transmit the slip further down the crystal but overall have no effect on the eventual plasticity generation around the indenter (figure 8).

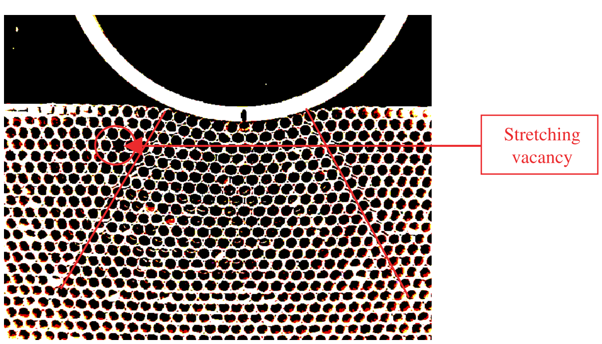

Figure 4. Atom movements are visible here (the two drawn lines) and the vacancy, located in the tension zone of the crystal, is stretching.

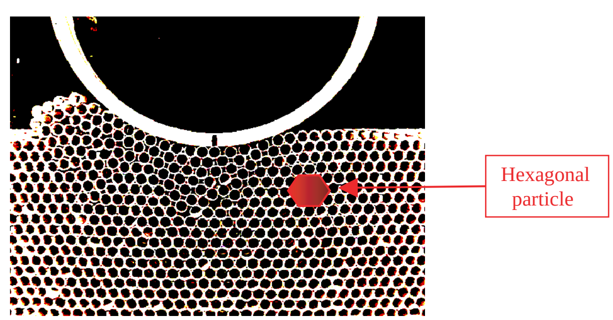

Figure 7. Atom movements are more on the side opposite to the particle placement. The presence of the particle seems to suppress plastic deformation of the crystal at its own side.

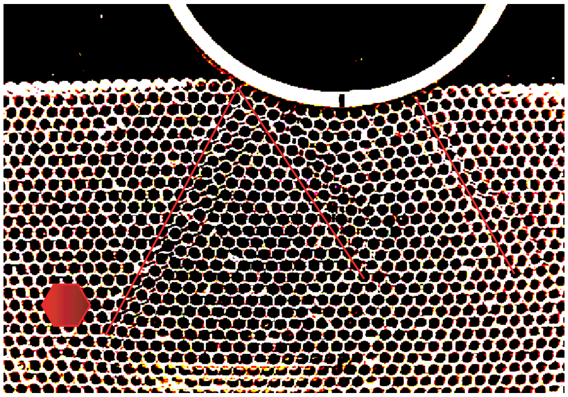

Figure 8. Transmission of slip further down the crystal due to the presence of a particle.

3.3 Interstitials

Interstitials in the compression zone cause atom movements below it (figure 9). This is similar to the particle effect. Also, interstitials present anywhere in the array locally disturb the close-packed structure and therefore act as sites for plasticity inception (figures 10 and 11). The strong effect of interstitials on the initiation of plasticity locally at their sites has been observed using computer atomistic simulations by one of the authors [14]. In this referenced study on a thin sheet, i.e. a 2D model, of a close-packed crystal was stretched in tension. A self-interstitial in the model repeatedly served as a nucleation site for plasticity or dislocations in an otherwise defect-free crystal.

3.4 Flat indenter

Upon flat indentation and before plasticity, slip lines can be clearly observed in the array (figure 12). This observation is consistent with the slip lines discussed in [13] for indentation of a material using a flat slab. Upon further indentation, a noticeable curling of atoms at the indenter edges is observed (figure 13). This curling might be an indicator of built-up rigid-body rotation at this location during the elastic deformation stages.

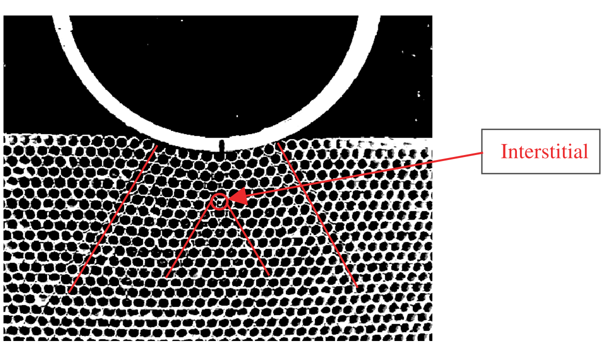

Figure 9. An interstitial placed in the compression zone induces atom movement beneath it.

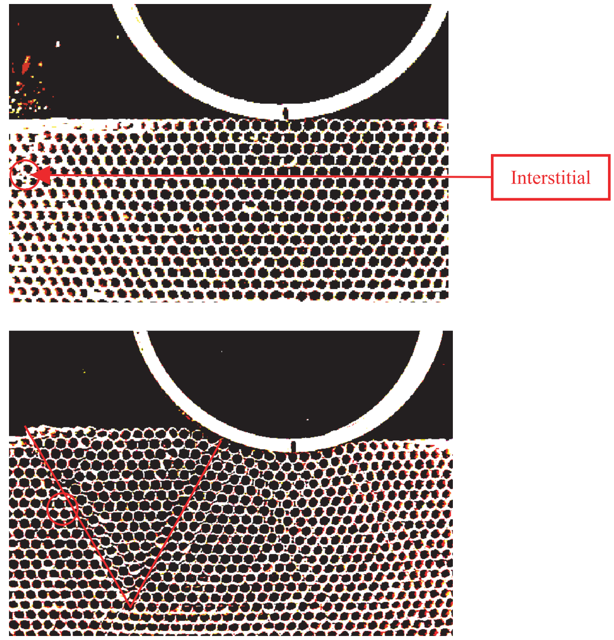

Figure 10. (a) The initial position of an interstitial just before indenting the array. (b) A whole triangle containing the interstitial slipped with one of the slip lines being a main slip direction identified in figure 1.

4. Comparison of straw model to computer simulations

A computational domain was used as a 2D finite-element model similar to our straw model. Although this is continuum-based modeling, insight into the indentation-induced mechanical fields can be gained in an

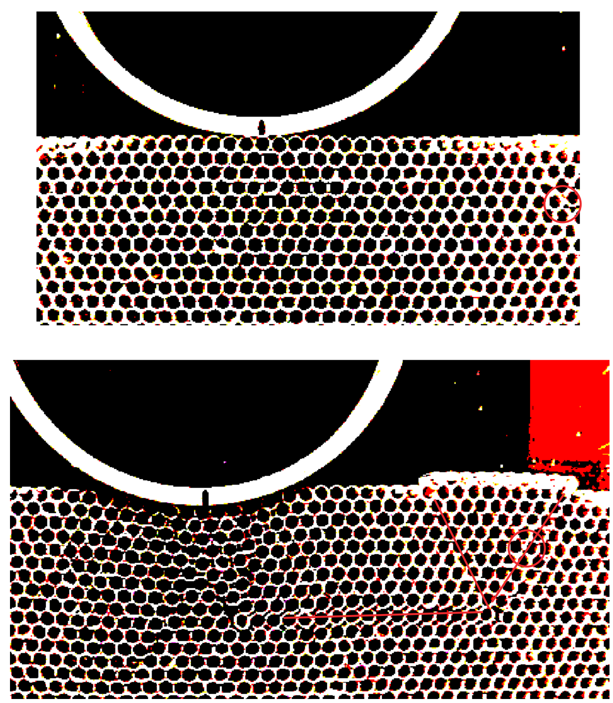

Figure 11. (a) An interstitial initially at the 5th row and 20th column (from the indentation axis). (b) A whole triangle, containing the interstitial, slips although the interstitial is *far away* from the indenter.

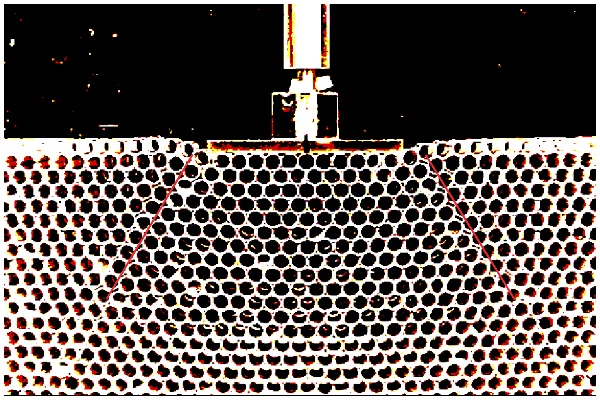

Figure 12. Typical slip lines observed with flat slab indentation.

unambiguous manner. In simulating the indentation, only half of the indenter/specimen combination was used because of symmetry. During indentation, the bottom boundary was allowed to slip tangentionally. The top boundary was not constrained except when a contact with the rigid indenter was established, a coefficient of friction of 0.1 was imposed. The left boundary was the symmetry axis and the right-hand boundary was free to move vertically but constrained horizontally. A total of 14,400 four-noded bilinear elements were used. The analyses were based on the plane stress formulation. The elements are taken to be linearly elastic with a Young's modulus (E) value equaling 0.42 MPa and a Poisson's ratio (ν) of 0.45. These two values were measured experimentally for the array of straws by performing compression tests on a rectangular block. The finite-element software ABAQUS [15] was used in our modeling.

Contour plots for pressure were obtained using the post-processor (figure 14) where the pressure P is defined as

$$P = \frac{-\mathrm{trace}(\boldsymbol{\sigma})}{3} \tag{1}$$

where $\boldsymbol{\sigma}$ here is the stress, (second-rank tensor) at a material point. A positive P-value would indicate compression and a negative value would indicate tension. It was observed in the experiments (figures 2 and 4) that vacancies squashed in a compression zone and stretched or enlarged in a tension zone. Those compression and tension zones and their extent were not clearly discernible from the experimental images.

The performed finite-element simulations can help better identify these zones. Comparing figure 14 to figures 2 and 4, it can be seen that the vacancy in figure 2 was under compression and the one in figure 4 was under tension. Given this corroboration, the phenomena of squashing or enlarging vacancies can be easily understood.

Using a flat indenter tip, in the above computer simulation model, with same boundary conditions and material property values, we obtained the pressure contour plot in figure 15. This picture is similar to the one obtained for the circular indenter (figure 14) in terms of the location of the compression and tension zones.

The state of stress $\boldsymbol{\sigma}$ at a material point can be decomposed into two components as follows:

$$\boldsymbol{\sigma} = \boldsymbol{\sigma}_{\mathbf{m}} + \boldsymbol{\sigma}_{\mathbf{d}} \tag{2}$$

where $\boldsymbol{\sigma}_{\mathbf{m}}$ is the mean stress tensor and is representative of the pressure P and $\boldsymbol{\sigma}_{\mathbf{d}}$ is the deviatoric stress tensor and is representative of the amount of local shearing. The pressure P is related to dilatation or volumetric strain (e.g. the squashing or stretching of vacancies). On the other hand, $\boldsymbol{\sigma}_{\mathbf{d}}$ is related to shear strain in the material.

Based on this and by examining the P contour plot in figure 15, one can see that the overlaid dashed line delineates positive and negative pressure and hence traces the zero pressure points. At these material points, the state of stress is dominated by shearing which is corroborated by the experimental image in figure 12.

The effect of vacancies on the deformation of a nanoindented material was studied using computer

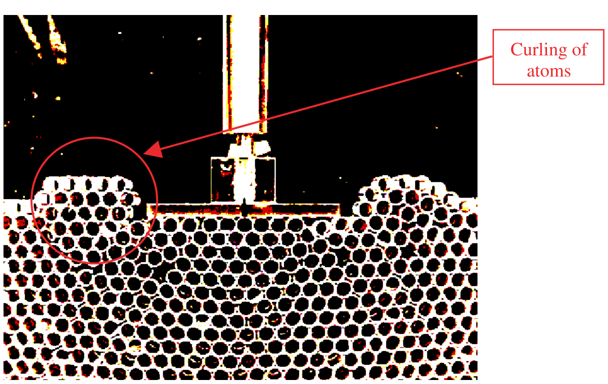

Figure 13. Curling of atoms at the edge of a flat indenter.

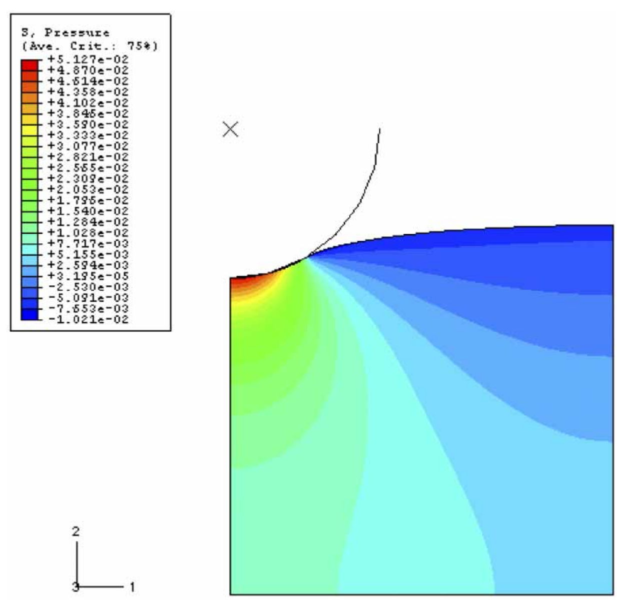

Figure 14. Pressure contour plot for a circular indenter showing regions of compression (under the indenter) and tension (away from the indenter and to the right).

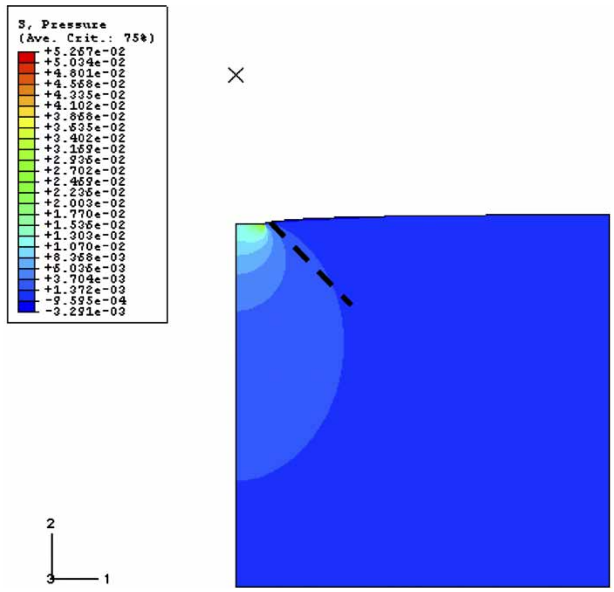

Figure 15. Pressure contour plot for a flat indenter showing regions of compression and tension as well as a trace of zero pressure (indicated by the dashed line).

atomistic simulations by our research group [11]. This was done by assigning a null potential to the atoms occupying select locations. Annihilation of vacancies by atomic row slip was one of their observations and conforms to our straw model (figures 2 and 3).

As a side note, in order to exactly quantify the interatomic force between any two straws as a function of their spacing, delicate tension/compression tests can be performed for this purpose by pulling away/pushing on these straws in a tensile/compression testing machine. Such a machine needs to be capable of resolving very small forces and synchronously relating them to the spacing. Rate effects on the force-spacing curve can be easily quantified this way by changing the pulling/pushing rates. Such quantification can in turn be utilized into quasi-static computer atomistic simulation modeling (such as those performed by our research group) to arrive at quantitative comparisons between the two methodologies.

Indentation response of a heterogeneous material system consisting of hard particles and a soft matrix within the 2D framework was also done previously by our research group [12]. In the indentation test, severe plastic flow is concentrated in the region directly below the indentation, outside of which the material still behaves elastically. This again conforms to our straw model observation containing a hexagonal particle in a softer matrix (figure 6).

Also, tensile stretching of a 2D model crystal was computationally studied using molecular statics by [14]. It was reported that the incorporation of an initial point defect (interstitial) is able to trigger atomic row slip in a repetitive manner. This again conforms to our straw model on the strong effect solute atoms have on triggering plasticity even though our model was loaded in compression via an indenter and not stretched in tension (figures 9–11).

5. Conclusions

From this work, we conclude that our straw model is capable of simulating defected crystalline structures. The observations from the model were corroborated with computer simulation results. The other main conclusions were that interstitials and particles had a strong effect on the indentation-induced plasticity. Vacancies do not seem to have much effect on the overall plasticity picture and get plugged in the compression zone early during deformation.

References

[1] S. Mukherjee, S. Murray, T. Khraishi, Y.-L. Shen. A straw model simulating nanoindentation. *Mol. Simul.*, (2006) (in press).
[2] W.L. Bragg, J.F. Nye. A dynamic model of a crystal structure. *Proc. R. Soc. Lond. A*, **190**, 474 (1947).
[3] A. Gouldstone, K.J. Van Vliet, S. Suresh. Simulation of defect nucleation in a crystal. *Nature*, **411**, 656 (2001).
[4] R.W. Leger, Y.-L. Shen, T.A. Khraishi. Defect nucleation during nanoindentation: an atomistic analysis. *J. Comput. Theor. Nanosci.*, **1**, 259 (2004).
[5] K.J. Van Vliet, S. Suresh. Simulation of cyclic normal indentation of crystal surfaces using bubble raft model. *Philos. Mag. A*, **82**, 1993 (2002).
[6] K.J. Van Vliet, J. Li, T. Zhu, S. Yip, S. Suresh. Quantifying the early stages of plasticity through nano-scale experiments and simulations. *Phys. Rev. B*, **67**, 104104 (2003).
[7] G. Das, S. Ghosh, S. Ghosh, R.N. Ghosh. Material characterization and classification on the basis of material pile-up surrounding the indentation. *Mater. Sci. Eng. A*, **408**, 158 (2005).
[8] D.F. Bahr, W.W. Gerberich. Plastic zone and pileup around large indentations. *Metall. Mater. Trans. A*, **27**, 3793 (1996).
[9] A. Gouldstone, H.-J. Koh, K.-Y. Zeng, A.E. Giannakopoulos, S. Suresh. Discrete and continuous deformation during nanoindentation of thin films. *Acta Mater.*, **48**, 2277 (2000).
[10] Z.-H. Xu, J. Ågren. An analysis of piling-up or sinking-in behavior of elastic–plastic material under a sharp indentation. *Philos. Mag.*, **84**, 2367 (2004).
[11] R.W. Leger. Multiscale simulation of defect mechanism in crystalline materials. PhD Dissertation, University of New Mexico (2004).
[12] Y.-L. Shen, Y.L. Guo. Indentation modeling of heterogeneous materials. *Model. Simul. Mater. Sci. Eng.*, **9**, 391 (2001).
[13] M.F. Ashby, R.H. Jones. *Engineering Materials*, p. 113, Butterworth-Heinemann, Oxford (1996).
[14] Y.-L. Shen. On the atomistic simulation of plastic deformation and fracture in crystals. *J. Mater. Res.*, **19**, 973 (2004).
[15] ABAQUS version 6.5-1, Hibbit, Karlson and Sorensen, Providence, RI (2005).